Journal of the American Heart Association

ORIGINAL RESEARCH

Gelatin Methacryloyl Bioadhesive Improves Survival and Reduces Scar Burden in a Mouse Model of Myocardial Infarction

Leon M. Ptaszek, MD, PhD*; Roberto Portillo Lara, PhD*; Ehsan Shirzaei Sani, BS; Chunyang Xiao, PhD; Jason Roh, MD; Xuejing Yu, MD, PhD; Pablo A. Ledesma, MD; Chu Hsiang Yu, PhD; Nasim Annabi, PhD†; Jeremy N. Ruskin, MD†

BACKGROUND: Delivery of hydrogels to the heart is a promising strategy for mitigating the detrimental impact of myocardial infarction (MI). Challenges associated with the in vivo delivery of currently available hydrogels have limited clinical translation of this technology. Gelatin methacryloyl (GelMA) bioadhesive hydrogel could address many of the limitations of available hydrogels. The goal of this proof-of-concept study was to evaluate the cardioprotective potential of GelMA in a mouse model of MI.

METHODS AND RESULTS: The physical properties of GelMA bioadhesive hydrogel were optimized in vitro. Impact of GelMA bioadhesive hydrogel on post-MI recovery was then assessed in vivo. In 20 mice, GelMA bioadhesive hydrogel was applied to the epicardial surface of the heart at the time of experimental MI. An additional 20 mice underwent MI but received no GelMA bioadhesive hydrogel. Survival rates were compared for GelMA-treated and untreated mice. Left ventricular function was assessed 3 weeks after experimental MI with transthoracic echocardiography. Left ventricular scar burden was measured with postmortem morphometric analysis. Survival rates at 3 weeks post-MI were 89% for GelMA-treated mice and 50% for untreated mice ($P=0.011$). Left ventricular contractile function was better in GelMA-treated than untreated mice (fractional shortening 37% versus 26%, $P<0.001$). Average scar burden in GelMA-treated mice was lower than in untreated mice (6% versus 22%, $P=0.017$).

CONCLUSIONS: Epicardial GelMA bioadhesive application at the time of experimental MI was performed safely and was associated with significantly improved post-MI survival compared with control animals. In addition, GelMA treatment was associated with significantly better preservation of left ventricular function and reduced scar burden.

Key Words: Bioadhesive ■ myocardial fibrosis ■ myocardial infarction

Currently available pharmacological and mechanical treatments for acute myocardial infarction (MI) are limited in their ability to prevent cell injury and death and associated inflammation.[1–5] Consequently, clinically significant myocardial fibrosis can be found even in patients who receive state-of-the-art treatment for acute MI.[6–8] Fibrosis-related disruption of myocardial architecture is responsible for the most common clinical sequelae of MI, including left ventricular (LV) contractile dysfunction and susceptibility to life-threatening ventricular arrhythmias and sudden cardiac death.[9,10]

Hydrogels are 3-dimensional (3D) hydrophilic polymer networks capable of absorbing large amounts of water to form a suitable environment for cellular growth.[11,12] Direct application of hydrogels to

CLINICAL PERSPECTIVE

What Is New?
- Gelatin methacryloyl (GelMA) bioadhesive hydrogel is nontoxic, biocompatible, and biodegradable.
- GelMA bioadhesive hydrogel can be delivered to the epicardial surface of the heart in liquid precursor form and polymerized in situ using visible-spectrum light, and the elastic properties of GelMA can be "tuned" to match the elasticity of native heart tissue.
- Application of GelMA bioadhesive hydrogel to the surface of a mouse heart at the time of experimental myocardial infarction was safe and was associated with reductions in post–myocardial infarction scar formation and mortality as well as preservation of left ventricular systolic function.

What Are the Clinical Applications?
- Epicardial application of GelMA bioadhesive hydrogel is safe and has the potential to reduce scar formation and preserve ventricular function in the setting of acute ischemic injury.
- GelMA bioadhesive hydrogel may serve as a biocompatible, biodegradable, sustained-release platform for the delivery of therapeutic agents to the heart.

Nonstandard Abbreviations and Acronyms

CD	cluster of differentiation
CF	cardiac fibroblast
DPBS	Dulbecco's phosphate-buffered saline
GelMA	gelatin methacryloyl
LV	left ventricular
MI	myocardial infarction
TTE	transthoracic echocardiography

the heart has been proposed as an adjunct to existing treatments for acute MI, with the goal of reducing myocardial fibrosis and adverse LV remodeling after MI.[13] Hydrogels could potentially modulate the post-MI injury response by providing biomimetic mechanical support to the infarcted, weakened tissue. They can also serve as vehicles for the delivery of therapies aimed at myocardial preservation and regeneration, including cells, proteins, nucleotides, and small molecules.[14–18] Recent advances in hydrogel polymerization chemistry have produced several formulations that can be efficiently crosslinked in vivo. These hydrogels can be applied to target organs in liquid form and crosslinked into solid form within the target organ. Application of hydrogel in liquid form could facilitate the development of less invasive delivery techniques than are required for delivery of pre–crosslinked (solid) hydrogels.[17,19]

Controlled polymerization of liquid hydrogel precursors in vivo is potentially challenging.[20] Chemical and enzymatic crosslinking strategies can lead to uncontrolled polymerization, which can compromise both the mechanical integrity of the scaffold and its ability to adhere to the target tissue.[21] Incomplete polymerization of hydrogel can also lead to leakage of unreacted components of the precursor solution into nontarget organs. Adjustment of the chemical/enzymatic polymerization conditions to produce more rapid polymerization may offset this risk, but may then result in other problems, such as polymerization within the equipment used to deliver the hydrogel. In addition, rapid polymerization can lead to undesirable mechanical properties, undesirable drug release kinetics, or both. Complete polymerization and tissue adhesion are particularly important in the context of the heart, as cardiac motion can lead to detachment and migration of incompletely polymerized hydrogel precursor.[22] Photoinitiation has emerged as an attractive alternative to chemical/enzymatic polymerization because it provides precise temporal and spatial control over the crosslinking process.[23,24] In addition, this approach allows for facile adjustment of the physical properties of the hydrogel (eg, elasticity and stiffness) to match those of the target tissue. Crosslinking of hydrogels through exposure to ultraviolet light has been described.[21] Although ultraviolet light has been previously shown to induce efficient crosslinking of hydrogels in vivo, the clinical use of ultraviolet light has been limited because of the DNA damage associated with ultraviolet light exposure, and the associated increase in the risk of cancer.[25]

The hydrogel system described in this study is based on the naturally derived biopolymer, gelatin, which can be modified to form photo–crosslinkable gelatin methacryloyl (GelMA). Gelatin was selected as the foundation of this system because it is highly biocompatible and biodegradable. In addition, through photopolymerization, we can adjust the rate of GelMA degradation so that GelMA is present during the time window needed for post-infarct injury repair, typically within 2 weeks of the initial event. GelMA hydrogel has been optimized to be photo–crosslinked through exposure to visible light (450–550 nm).[26–28] Visible light crosslinking has been shown to retain the advantages of ultraviolet-based crosslinking (strong adhesion to tissue, rapid and controlled polymerization), without the adverse effects associated with exposure to ultraviolet light.[29] In addition, visible-spectrum light provides comparatively deeper tissue penetration than ultraviolet light, with lower energy.[30] The physical

properties of GelMA bioadhesive, such as elastic modulus and in vivo half-life, can be adjusted through changes in the concentration of precursors and the duration of photo–crosslinking.[26] Together, these features enhance the suitability of this visible light photo–crosslinking strategy for clinical applications.

The GelMA hydrogel system relies on the use of eosin Y as a chemical photoinitiator. Although several photoinitiators have been used with visible light-activated systems, eosin Y is the only one that has been approved by the US Food and Drug Administration for clinical use.[31] Moreover, the irradiation times required to achieve polymerization using eosin Y are shorter than other photoinitiator systems. This increases the efficiency of crosslinking and minimizes the risk of potential leakage of unreacted hydrogel precursor. Shorter irradiation time may also enhance the viability of cells incorporated within the hydrogel.[32]

This proof-of-concept study was designed to assess the cardioprotective impact of visible light crosslinked GelMA bioadhesive applied to the epicardial surface of the heart at the time of experimental MI in mice. Epicardial application was used to avoid the risks of delivery by intramyocardial injection, including cardiac injury and systemic spread of hydrogel. In this study, the bioadhesive precursors were delivered to the epicardial surface in liquid form immediately after creation of an experimental MI. GelMA prepolymer was photo-crosslinked immediately after epicardial application with visible-spectrum light. Several post-MI outcomes were measured, including mortality rate, LV contractile function, and LV scar burden.

METHODS

Data will be made available at the Harvard Dataverse and will be accessible via the Dataverse site.

Synthesis and Chemical Characterization of GelMA Bioadhesives

GelMA hydrogel was synthesized as described previously.[33] Gelatin from porcine skin (Sigma-Aldrich) was dissolved in Dulbecco's phosphate-buffered saline (DPBS; Gibco) to a final concentration of 10 g/100 mL. A total of 8 mL of methacrylic anhydride (Sigma-Aldrich) was then added to react with gelatin for 3 hours at 60°C. This solution was then diluted 3-fold with DPBS, dialyzed against distilled water for 7 days, and lyophilized. The bioadhesive precursor solution (10% (w/v)) was then prepared in DPBS containing 1.88% (w/v) triethanolamine (Sigma-Aldrich) and 1.25% (w/v) of N-vinylcaprolactam (Sigma-Aldrich). Eosin Y was dissolved separately in DPBS to produce a 0.5 mmol/L solution. The final bioadhesive hydrogel was prepared by using 10% (w/v) GelMA,

1.5% triethanolamine, 1% N-vinylcaprolactam, and 0.1 mmol/L eosin Y. The bioadhesive precursor was warmed up to 37°C and was then exposed to blue-green light (100 mW/cm²; xenon source from Genzyme Biosurgery) in the 450- to 550-nm range for 1, 2, and 4 minutes to form crosslinked hydrogels. The distance between the light source and the target was 1 cm for all experiments. The formation of the crosslinked hydrogel network and estimation of the degree of cross-linking were determined through proton nuclear magnetic resonance (HNMR) analysis using a Varian Inova 500 nuclear magnetic resonance spectrometer, as described previously.[34]

In Vitro Swelling and Degradation of GelMA Bioadhesive

To determine GelMA bioadhesive water uptake (swelling), the hydrogels were synthesized and their weights were measured after incubation in DPBS at 37°C for 48 hours. The hydrogels were then lyophilized, and the weights were remeasured. The swelling ratio was defined as the hydrated weight divided by the dry weight (n=6).

To determine the in vitro degradation rate, the hydrogels were freeze dried, weighed, and incubated in 1 mL of DPBS at 37°C for 14 days. The samples (retrieved at days 1, 4, 7, 10, and 14 post-incubation) were freeze dried and weighed. The degradation ratio of the hydrogels was calculated by dividing the initial dry weight by the dry weight after incubation (n=6).

Mechanical Characterization of GelMA Bioadhesive

The elastic moduli of the hydrogels were determined as described previously.[35] Hydrogels were synthesized as described above using rectangular (14×5×1 mm) molds. Uniaxial tensile tests were performed on hydrogels placed between 2 pieces of double-sided tape within the tension grips of an Instron 5542 mechanical tester (n=4). Hydrogels were extended at a rate of 1 mm/min until failure. The stress-strain curves were used to calculate the elastic moduli.

Burst Pressure and Adhesive Strength of GelMA Bioadhesive

Burst pressure was determined on the basis of procedures described previously (n=4).[36] Explanted rat hearts were used for burst pressure and adhesion tests. The LV was punctured and sealed with either the GelMA bioadhesive or a commercially available, polyethylene glycol–based sealant (Coseal; Baxter). A small catheter, connected on one end to a syringe pump with a pressure sensor, was introduced into the LV. Air was injected into the LV at 0.5 mL/s until rupture. Pressure at the time of LV rupture was recorded.

The adhesive strength of the hydrogels was determined on the basis of a modified American Society for Testing and Materials F2458-05 standard (n=4).[34] Rat hearts were washed, and the blood vessels and the atria were removed. The ventricles were then cut into sections (1×1 cm) and immersed in DPBS. The samples were then glued onto glass slides and joined together using either GelMA bioadhesive or Coseal. Samples (n=6) were stretched at a rate of 1 mm/min. Adhesive strength was measured at the point of tearing.

Scanning Electron Microscopy

GelMA bioadhesives were polymerized on the surface of explanted rat hearts, as described above, to visualize the interface between the tissue and the scaffold. The samples were then lyophilized, coated, and imaged with a Hitachi S 4800 Scanning Electron Microscope (SEM), as described previously.[34,35]

In Vitro Cytocompatibility of GelMA Bioadhesives

Cytocompatibility of GelMA bioadhesive was evaluated through 3D encapsulation of freshly isolated rat cardiomyocytes (CMs) and cardiac fibroblasts (CFs) at a ratio of 2:1 (CMs:CFs), within the hydrogel, as described previously.[35] CMs and CFs were isolated from rat heart on the basis of the procedures explained in our previous studies.[37–39] The cells were then encapsulated at $1.8×10^7$/mL density inside the hydrogel, as described previously.[26,39] Cell viability within the hydrogel was evaluated using a commercial live/dead kit (Invitrogen) and fluorescent staining against F-actin/cell nuclei and sarcomeric α-actinin, as described previously.[26,39]

Experimental MI

In vivo experiments were conducted on 40 C57BL6 mice (Charles River Laboratories) at ≈12 to 15 weeks of age. The study protocol was reviewed and approved by the Subcommittee for Research Animal Care at the Massachusetts General Hospital, according to the American Association of Laboratory Animal Care standards for proper research animal care. Animals were brought to the procedure suite, general anesthesia was induced, and endotracheal intubation was performed. Vital signs were monitored continuously. After intubation, MIs were created in the following manner. The heart was exposed through a left anterior thoracotomy. The pericardial sac was opened, and the anterior interventricular artery was visualized. A 6.0 Prolene suture (Ethicon) was used to ligate this vessel at its midportion, one half of the distance between the base and the apex of the heart. Blanching of the affected tissue (distal segment of the anterior wall) was visualized in all animals. The thoracotomy was then closed, and the animal was monitored until it recovered from anesthesia.

Bioadhesive Application and Photo–Crosslinking

Immediately after ligation of the anterior interventricular artery, ≈5 µL of the liquid bioadhesive precursor was placed on the epicardial surface of the affected myocardium in 20 mice. Hydrogel precursor was immediately exposed to light for 4 minutes. Twenty control mice received no additional intervention at the time of experimental MI.

Echocardiography

M-mode transthoracic echocardiography (TTE) was performed on all mice ≈3 weeks after experimental MI (Vivid E90; General Electric). All TTEs were performed on conscious mice. LV wall thickness and chamber dimensions were measured offline using EchoPACS software (GE Healthcare, version 201). Fractional shortening of the LV was calculated using the following formula: fractional shortening=[(LV end-diastolic diameter–LV end-systolic diameter)/LV end-diastolic diameter]×100.

Morphometric Analysis to Assess Myocardial Scar Burden

Mouse hearts were explanted postmortem, fixed in 4% formalin solution, and embedded in paraffin blocks. Short-axis sections of the ventricles were created and then stained with Masson's trichrome. For each heart, 5 equally spaced sections were used to calculate fibrosis ratio, as described previously.[40,41]

Sample Size Calculation

The primary end point of the study was reduction in LV scar burden associated with GelMA treatment, as observed at the end of the prescribed postinfarct survival period. The estimated likelihood of successfully observing a difference in LV function between GelMA-treated and untreated mice was 50%. This estimation was based on our prior experience with pharmacologic, antifibrotic interventions in this mouse infarct model (Jason Roh MD (JR) and Chunyang Xiao PHD (CX), unpublished data, 2016). On the basis of this assumption, 6 iterations (in each study group) were required to achieve a 98% likelihood of making a successful observation. The estimated likelihood that a mouse survived the procedure and the postinfarct survival period was estimated to be ≈33%, thus increasing the total number of mice in each group to 18. Estimation of survival was also based on our prior experience with the model, in which intraprocedural mortality ranged between 5% to 10% and postprocedural mortality ranged between 30% and 50% (Jason Roh MD (JR) and Chunyang Xiao PHD (CX), unpublished data, 2016). To accommodate unexpected issues, a total sample size of 20 (for each group) was selected.
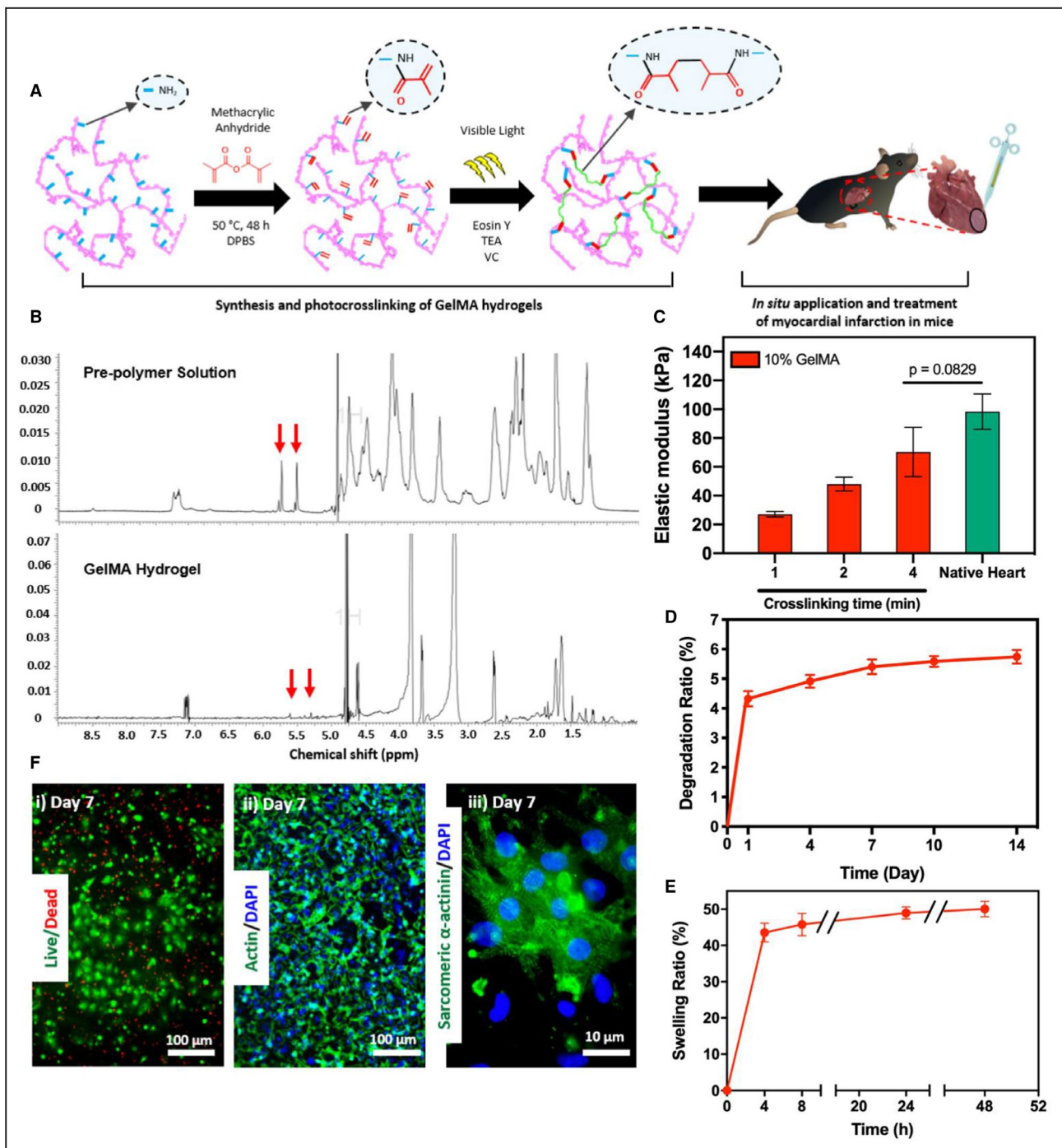
Figure 1. Synthesis and in vitro characterization of gelatin methacryloyl (GelMA) bioadhesive hydrogel.
A, Schematic of the synthesis and in vitro photo–crosslinking strategy of the bioadhesive hydrogel. **B**, ^{1}H nuclear magnetic resonance (500 MHz; dimethyl sulfoxide (DMSO)-d6) spectra of GelMA precursor and crosslinked GelMA bioadhesive hydrogel. **C**, Elastic moduli of GelMA bioadhesive hydrogel produced with 10% (w/v) total polymer concentrations at different visible light exposure times, compared with native myocardium (n=4). In vitro degradation (**D**) and swelling ratios (**E**) of GelMA hydrogel (n=4). **F**, Representative images of (**i**) live/dead assay, and fluorescent staining against (**ii**) F-actin/4′, 6-diamidino-2-phenylindole (DAPI) and (**iii**) sarcomeric α-actinin using 3-dimensional (3D) encapsulated neonatal rat cardiomyocytes and cardiac fibroblasts inside the hydrogel at day 7 post-encapsulation. Data are shown as mean±SD. *P* values were determined by 1-way ANOVA, followed by Tukey's multiple comparisons test for **C**.

Statistical Analysis

One-way ANOVA was used to assess in vitro swelling and degradation of GelMA. Tukey's multiple comparisons test was used to assess the elastic modulus of GelMA produced with different crosslinking times. All pairwise comparisons of

intraoperative and post-MI mortality were performed with a χ^2 test. Differences in LV function (as measured by TTE) and scar burden (as measured by morphometric analysis) were compared with 2-sample T tests. All means are expressed with SD. Results are displayed using the Graphpad software package.

RESULTS

Visible light crosslinking generated a 3D hydrogel network (Figure 1A). Successful crosslinking was confirmed through HNMR analysis. The successful crosslinking of GelMA hydrogels via exposure to visible light was confirmed by the disappearance of the peaks at $\delta=5.3$ and 5.7 ppm on the spectra of the crosslinked hydrogel. These correspond to the methacrylated groups ($-C=CH_2$) on GelMA (Figure 1B). The degree of crosslinking was determined by measuring the change in the integrated areas under the peaks corresponding to un–crosslinked and crosslinked hydrogel. This comparison revealed that the degree of GelMA crosslinking was 92.9±2.24% after 4 minutes of exposure to visible light.

Physical Characterization of GelMA Bioadhesives

Mechanical properties of bioadhesives formed using different crosslinking times (1, 2, and 4 minutes) were evaluated. In addition, the mechanical properties of rat heart were measured and compared with synthesized hydrogels (Figure 1C). Rat hearts were used because mouse hearts were too small for this purpose. Hydrogels synthesized with a final concentration of 10% (w/v) GelMA and photo–crosslinked with 4 minutes of visible light exposure exhibited an elastic modulus not significantly different from that of native rat myocardium ($\approx$60 kPa, Figure 1C).[42] After 14 days of incubation, GelMA hydrogels exhibited a degradation ratio of 5.7±0.2% (Figure 1D), as well as a swelling ratio of 50.1±2.1% at 48 hours after incubation in DPBS (Figure 1E).

In Vitro 3D Cell Encapsulation in GelMA Bioadhesive

GelMA bioadhesives supported the growth and proliferation of 3D encapsulated CMs/CFs in vitro (Figure 1F). Viability of CMs/CFs in GelMA remained >90% up to 7 days post-encapsulation (Figure 1F-i). Fluorescent F-actin staining revealed that the cells could efficiently attach and spread across the bioadhesive scaffold (Figure 1F-ii). In addition, immunofluorescent staining revealed that GelMA could preserve the cardiac phenotype of 3D encapsulated CMs, as demonstrated by positive sarcomeric α-actinin expression 7 days after encapsulation (Figure 1F-iii).

Ex Vivo Burst Pressure and Adhesive Strength of GelMA Bioadhesive

The burst pressure of the GelMA bioadhesive (11.7±1.7 kPa) was significantly higher than that of Coseal (6.7±1.7 kPa). Burst pressures for both GelMA and Coseal were lower than intact heart burst pressure (30.0±2.3 kPa, Figure 2A). Adhesive strength was significantly higher for GelMA (21.2±3.8 kPa) than for Coseal (11.1±1.8 kPa, Figure 2B). The adhesiveness of GelMA hydrogel to the native myocardium was confirmed with SEM imaging of the hydrogel/tissue interface (Figure 2C). SEM images revealed the establishment of mechanical bonding between the bioadhesive scaffold and the tissue.

Effect of GelMA on Survival After Experimental MI

Experimental MI was generated by permanent ligation of the anterior interventricular artery in 40 mice (Figure 3A). In 20 of these mice, liquid GelMA precursor was applied to the epicardial surface of the affected area of the anterior wall of the LV, and 20 control mice were untreated at the time of MI. The GelMA precursor solution was photo–crosslinked by application of visible-spectrum light (Figure 3B). Intraprocedural mortality was 2 of 20 (10%) in both GelMA-treated and untreated mice (Table 1). The post-MI survival rate at 3 weeks was 89% among GelMA-treated mice and 50% among untreated control mice (Table 1, $P=0.011$). For all mice that did not survive the 3-week observation period, average post-MI survival was 4±2 days. Postmortem analysis was performed on all mice that did not survive the prespecified, 3-week end point. In all such cases, the postmortem analysis revealed evidence of LV myocardial rupture in the infarct territory with hemothorax (Figure 3C).

Effect of GelMA on LV Function After Experimental MI

TTE was performed in all surviving animals 3 weeks after experimental MI. Thickness of the anterior wall of the LV was measured at the midventricle for all animals, because this corresponded to the location of the infarcts. TTE analysis revealed that the average thickness of the anterior wall of the LV was significantly lower in untreated mice compared with GelMA-treated mice (0.58 versus
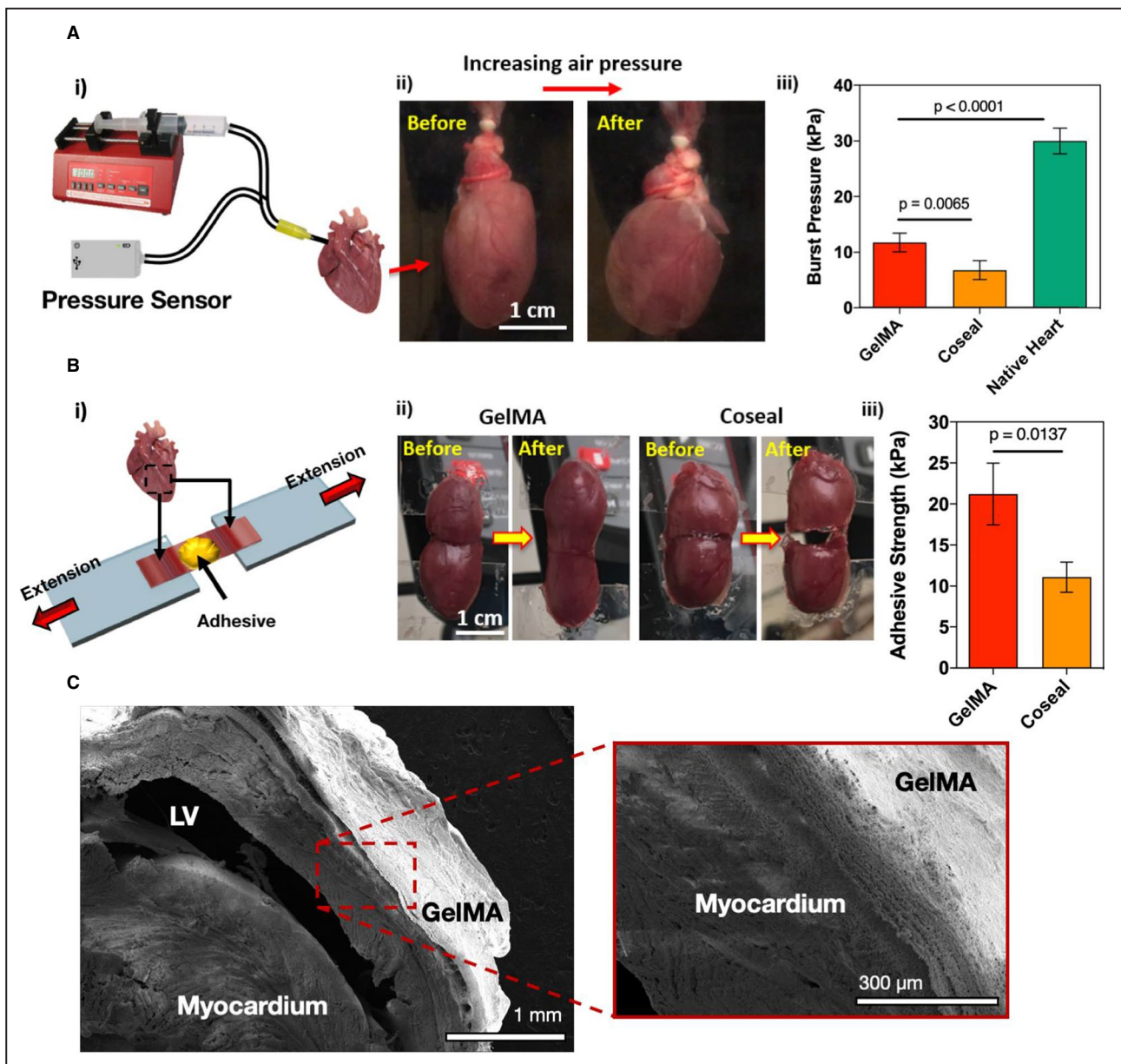
Figure 2. In vitro characterization of burst pressure and adhesive strength of gelatin methacryloyl (GelMA) bioadhesive hydrogel.
A, Burst pressure test on explanted rat hearts treated with GelMA bioadhesive (n=6) and the commercially available sealant Coseal (n=6). (**i**) Schematic of the modified standard test method for burst pressure, (**ii**) representative images of rat hearts before and after applying air pressure, and (**iii**) average burst pressure of GelMA hydrogels (10% [w/v]) compared with Coseal and a pristine heart. **B**, Wound closure test to measure the adhesive strength on isolated rat hearts treated with GelMA bioadhesive (n=6) and Coseal (n=6). (**i**) Schematic of the modified standard test method for wound closure, (**ii**) representative images of the wound closure test on samples from rat ventricles using GelMA and Coseal, and (**iii**) adhesive strength of GelMA hydrogels (10% [w/v]) compared with Coseal. **C**, Representative scanning electron micrographs from the interface between the ventricular myocardium and the GelMA hydrogels. Data are shown as mean±SD. *P* values were determined by 1-way ANOVA, followed by Tukey's multiple comparisons test, for **A** and **B**. LV indicates left ventricle.

0.86 mm, *P*<0.001; Table 2). Posterior wall thickness was not significantly different between the untreated and GelMA-treated mice (0.85 versus 0.89 mm, *P*=0.419). Representative images of the echocardiograms from which these measurements

were obtained are shown in Figure 4. The average LV end-diastolic diameter was not significantly different between the GelMA-treated and untreated mice; however, contractile function was significantly different between the 2 groups. Average
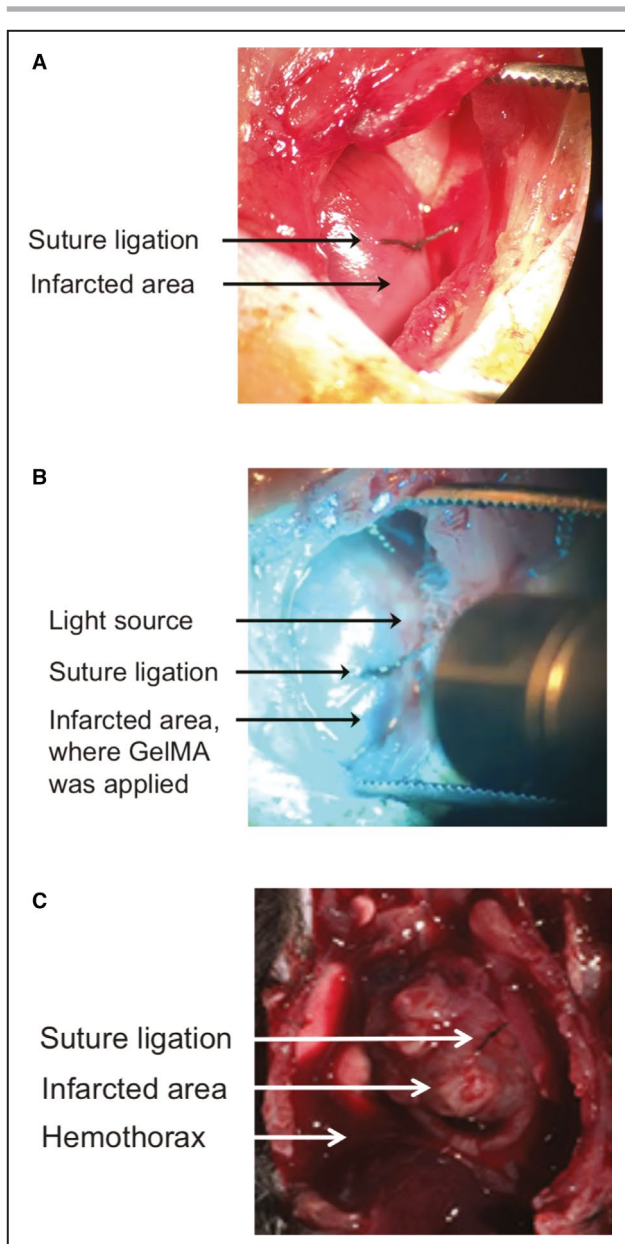
Figure 3. Experimental myocardial infarction (MI) and gelatin methacryloyl (GelMA) photo–crosslinking in situ.
A, View of the anterior wall of the left ventricle (LV) through a surgical thoracotomy. Placement of the suture ligation of the anterior interventricular artery is visible. The myocardium distal to the suture is blanched, consistent with ischemic injury. **B**, View of the anterior wall of the LV through a surgical thoracotomy. Suture ligation of the anterior interventricular artery can be seen as visible light is shone on the anterior LV wall immediately after the GelMA liquid precursor was applied to the area of injury in the anterior wall distal to the suture. **C**, Representative image of postmortem gross pathological characteristics in animals that did not survive the 3-week observation period after MI. An anterior view of the thoracic cavity is displayed. Location of the suture ligation on the anterior wall of the heart is visible, as is the region of post-MI injury. Presence of blood in the chest cavity is visible adjacent to the heart.

fractional shortening was significantly higher in GelMA-treated mice compared with untreated mice (37% versus 26%, *P*<0.001).

Table 1. Intraoperative and Postoperative Survival for Experimental MI Procedures

Variable	Untreated	GelMA Treated	*P* Value
No. of experimental MIs	20	20	…
Intraoperative mortality	2/20 (10)	2/20 (10)	1
Survival 3 wk after MI	9/18 (50)	16/18 (89)	0.011

Data are given as number/total (percentage), unless otherwise indicated. GelMA indicates gelatin methacryloyl; and MI, myocardial infarction.

Effect of GelMA Bioadhesive on LV Scar Burden After Experimental MI

Morphometric analysis was performed on Masson's trichrome-stained sections of the LV. Average transmural scar volume was expressed as a percentage of the total volume of LV myocardium. In GelMA-treated mice, the average scar volume was significantly smaller than the average scar volume in untreated mice (6±9% versus 22±10%, *P*=0.017; Figure 5A). Reduced LV scar burden in GelMA-treated mice was also apparent on visual inspection of stained sections (Figure 5B).

Effect of GelMA on Cellular Architecture of LV After Experimental MI

Immunofluorescent staining was performed to identify changes in cellular architecture associated with experimental MI. Differences between GelMA-treated and untreated mice were analyzed. In mice treated with GelMA, the expression of CM-associated markers sarcomeric α-actinin, cardiac troponin I, and connexin 43 was maintained within the infarcted area of the LV. A representative comparison is displayed in Figure 6A through 6C. This is consistent with preservation of

Table 2. Measurement of LV Size, Wall Thickness, and Contractile Function With TTE 3 Weeks After Experimental MI

Variable	Untreated (N=9)	GelMA Treated (N=15)	*P* Value
Anterior wall thickness, mm	0.58±0.13	0.86±0.11	<0.001
Posterior wall thickness, mm	0.85±0.17	0.89±0.11	0.419
LV end-diastolic diameter, mm	4.09±1.22	3.86±0.36	0.465
LV end-systolic diameter, mm	3.05±1.08	2.43±0.34	0.034
Fractional shortening, %	26±5	37±4	<0.001

All data presented as mean±SD. GelMA indicates gelatin methacryloyl; LV, left ventricular; MI, myocardial infarction; and TTE, transthoracic echocardiography.
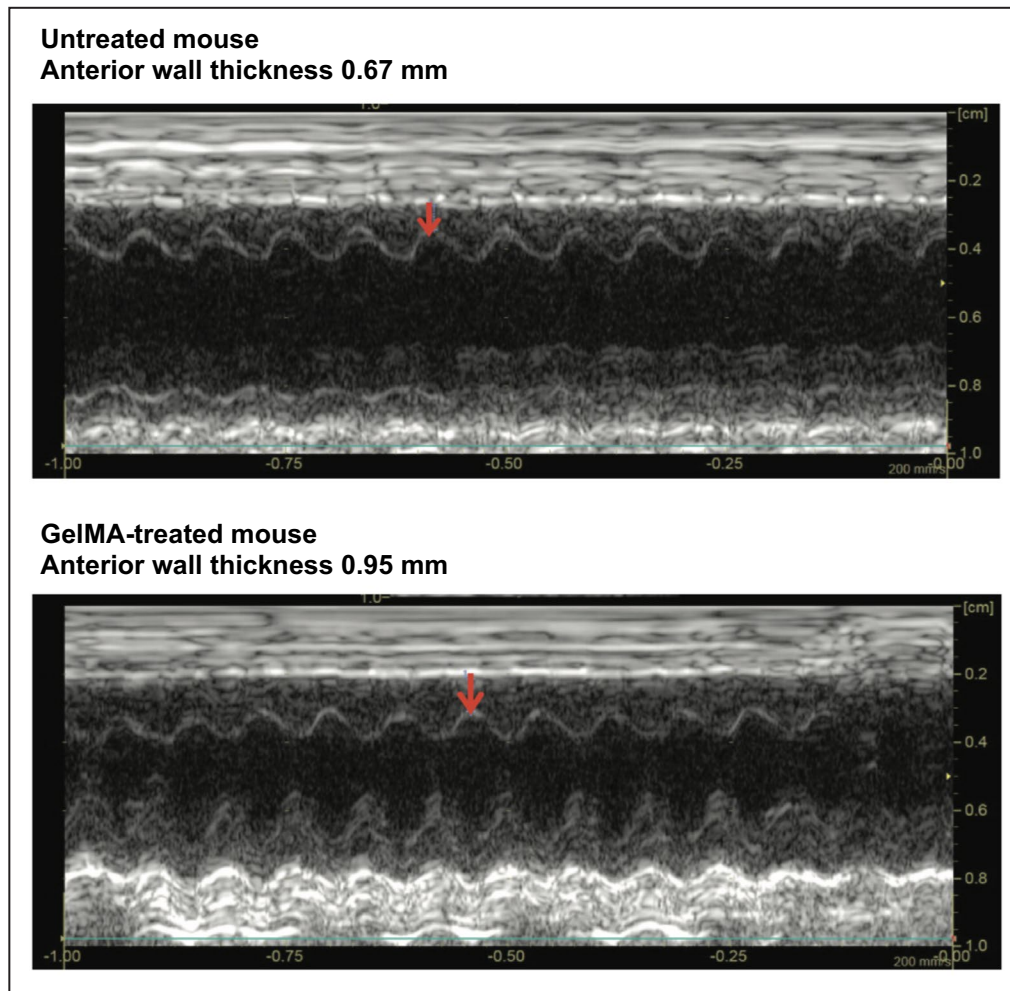
Figure 4. Transthoracic echocardiography after myocardial infarction.
M-mode echocardiograms in representative untreated (**top**) and gelatin methacryloyl (GelMA)–treated (**bottom**) mouse hearts. Measurement of anterior left ventricular wall thickness denoted by the location of the red arrow in each panel.

CMs within the infarcted territory for GelMA-treated mice. The expression of the endothelial marker CD31 was also observed at the site of MI in GelMA-treated mice, corresponding to improved vascularization as compared with untreated mice (Figure 6D). Immunofluorescent staining was also performed against surface markers for T cells (CD3) and macrophages (CD68) to assess inflammation in the infarcted territory. Expression of CD3 was not clearly different in untreated and GelMA-treated mice. A representative example is displayed in Figure 6E. Staining for CD68 was more distinct in untreated mice than in GelMA-treated mice (representative example in Figure 6F). This is consistent with reduction in MI-related inflammation in GelMA-treated mice. Together, staining for CMs, vascular endothelial cells, T cells, and macrophages indicates that GelMA hydrogel produced a reduction in the architectural disruption in myocardium without producing inflammation.

DISCUSSION

Development of a therapeutic hydrogel that is capable of adhering to a beating heart in vivo without causing toxic adverse effects presents multiple challenges.[43,44] Previously reported hydrogels and adhesives all possess limitations that limit their potential for use as therapeutic agents. For example, synthetic cyanoacrylate-based adhesives can be applied as liquid precursors and effectively crosslinked to selected tissues, but are too toxic for safe use on internal organs.[45,46] In addition, cyanoacrylate glues are more rigid than cardiac tissue, and may disrupt contraction and promote rupture.[47]

As distinct from cyanoacrylate-based adhesives, hydrogels based on naturally occurring biological molecules are generally nontoxic. For example, several fibrin-based adhesives have been shown to be biocompatible. The elasticity of fibrin-based adhesives is
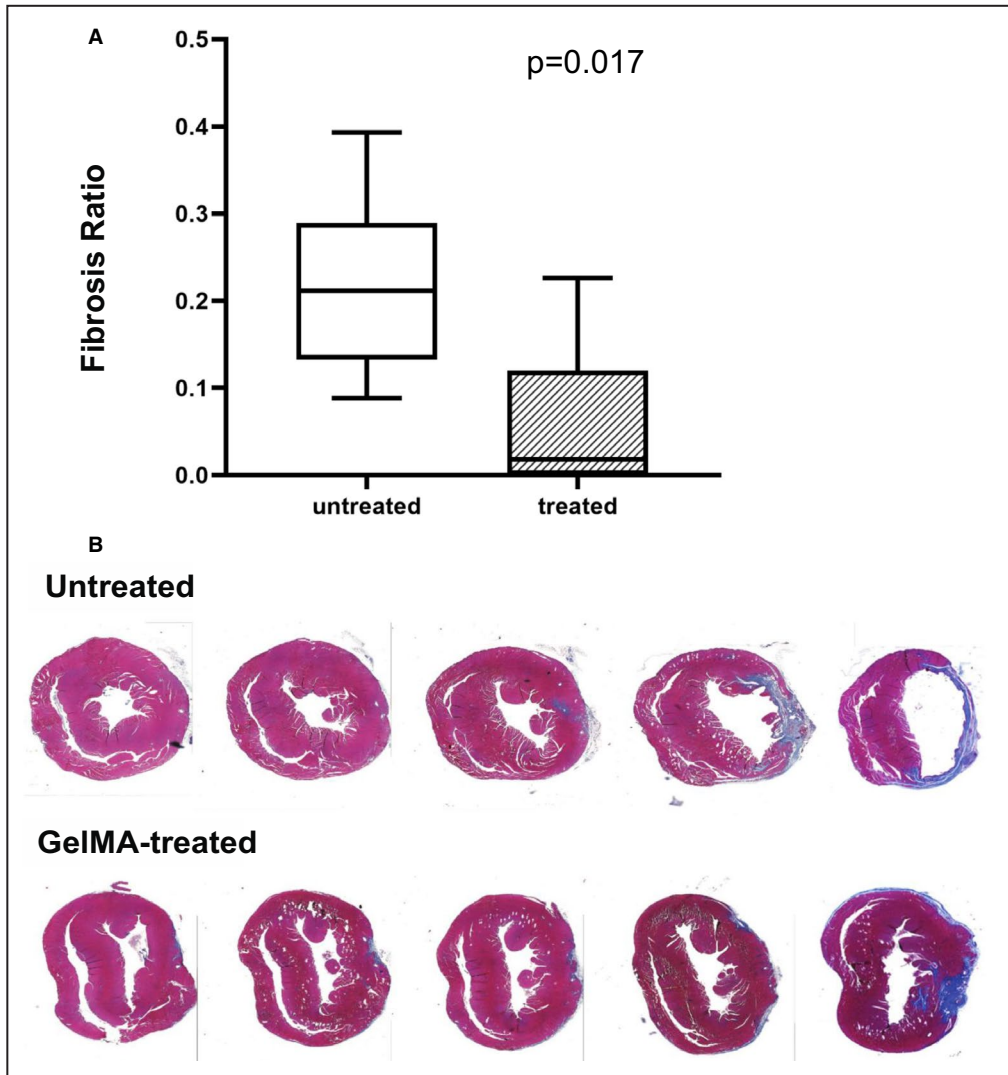
Figure 5. **Post–myocardial infarction scar burden in gelatin methacryloyl (GelMA)–treated vs untreated mice.**
A, Box plots representing the percentage of transmural left ventricular (LV) fibrosis in GelMA-treated and untreated mice. The box limits represent the first and third quartiles. The center line within each box represents the median value. Whiskers represent the most extreme data points within the 1.5× interquartile range. **B**, Representative series of short-axis Masson's trichrome-stained sections of the LV taken from untreated and GelMA-treated mice that survived the 3-week monitoring period. Viable myocardium is stained pink, and collagen (scar) is stained blue.

also closer to that of cardiac tissue than cyanoacrylates. Unfortunately, fibrin-based glues exhibit low adhesion to tissue, particularly when the tissue is wet.[48,49] Suboptimal tissue adhesion can lead to mechanically unstable hydrogel scaffolds that may detach from the heart during contraction. A gelatin-based sealant that exhibits better bonding to tissue has been described, but use of this sealant in the heart is limited by low elastic modulus and cytotoxicity.[49]

Photo–crosslinkable hydrogels have also been created from chemically modified biomolecules with the goal of improving tissue adhesiveness while retaining the biocompatibility and elasticity of naturally occurring biopolymers. These hydrogels can be delivered to tissue in liquid precursor form, with photo–crosslinking into solid form in situ. Application of previously reported photo–crosslinkable, adhesive hydrogels to the heart is limited by potentially dangerous adverse effects of the photo–crosslinking reaction. For example, a recently described silk fibroin gel is a nontoxic, elastic hydrogel based on naturally occurring silk fiber.[50] Although silk fibroin is fully biocompatible and biodegradable, it requires γ rays for photo–crosslinking. Delivery of liquid precursor to the target tissue with in vivo cross-linking
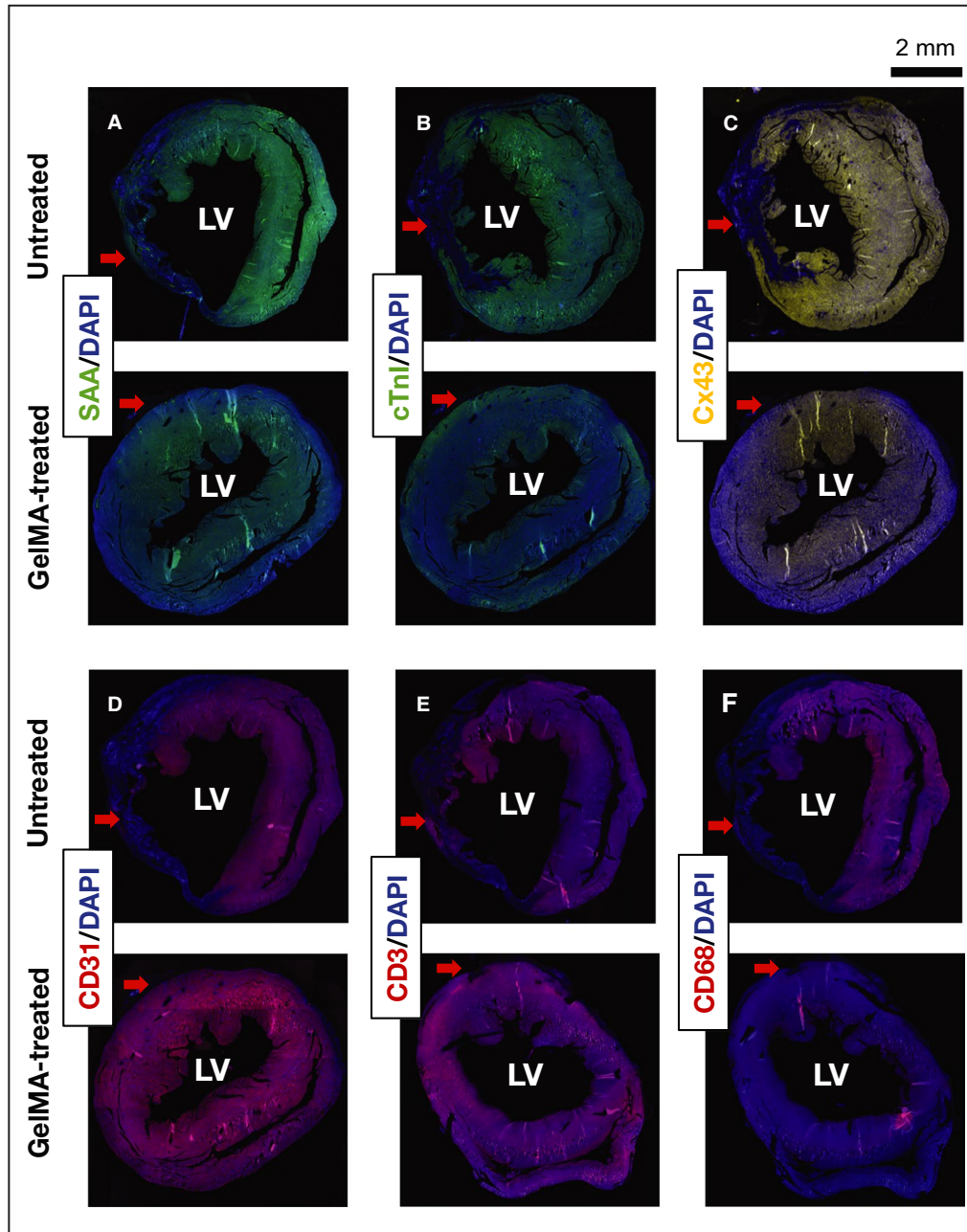
Figure 6. Immunofluorescent staining of short-axis sections from gelatin methacryloyl (GelMA)–treated and untreated mice.

Representative images of immunofluorescent staining of untreated and GelMA-treated hearts against sarcomeric α-actinin (SAA) (**A**), cardiac troponin I (cTnI) (**B**), connexin 43 (Cx43) (**C**), CD31 (**D**), CD3 (**E**), and CD68 (**F**). Samples were counterstained with 4′, 6-diamidino-2-phenylindole (DAPI). Red arrows indicate the area of the left ventricle (LV) affected by the ligation of the anterior interventricular artery leading to myocardial infarction.

is therefore associated with an unacceptably high risk of radiation-associated injury.[51] Other photo–crosslinkable hydrogels, including polyglycerol sebacate acrylate and methacryloyl-substituted tropoelastin, have been shown to adhere effectively to wet tissues.[52,53] Both polyglycerol sebacate acrylate and methacryloyl-substituted tropoelastin can be photo–crosslinked in vivo with an ultraviolet light source. Because of concerns about long-term risks of ultraviolet exposure, in vivo crosslinking of polyglycerol sebacate acrylate and methacryloyl-substituted tropoelastin is impractical. Although ex vivo crosslinking could be considered for these hydrogels, requirement that the hydrogel be applied as a preformed solid could limit clinical

applications. Because of the known disadvantages of ultraviolet crosslinking, in vivo comparisons between GelMA bioadhesive and ultraviolet-requiring hydrogel systems were not performed as part of this study.

The GelMA bioadhesive hydrogel described in this study was designed to address the limitations associated with previously reported hydrogels and adhesives. In this study, GelMA was demonstrated to be nontoxic, biocompatible (Figure 1F), and biodegradable (Figure 1D). The concentration of GelMA precursors and the duration of crosslinking time were "tuned" to produce a bioadhesive that would maintain structural integrity for at least 14 days after crosslinking. This time period was selected to provide structural support (and possibly deliver drug or cell therapies) during the post-MI healing period (Figure 1D).[53] GelMA was rapidly and efficiently photo–crosslinked in vitro using a visible-spectrum light source (Figure 1B).

The elastic modulus of crosslinked GelMA bioadhesive can also be "tuned" to match a target tissue. A previously described GelMA formulation was produced to have an elastic modulus that matches that of lung.[54] This previous version of GelMA, which was photo–crosslinked using an ultraviolet light source, used a 20% (w/v) polymer concentration. The GelMA formulation in the current study used a 10% (w/v) polymer concentration and produced a crosslinked bioadhesive whose elastic modulus was comparable to that of native mouse myocardium (Figure 1C).

The GelMA formulation described in this study also adheres strongly to the epicardial surface of the heart (Figure 2). Adhesion of GelMA to wet tissue was stronger than the adhesion reported for other adhesives, including the commercially available surgical sealant Coseal.[36] The strong adhesion of the scaffold to the tissue could be partly explained by the molecular entanglement between the hydrogel polymer chains and extracellular matrix proteins.[36] Infiltration of the extracellular matrix by the liquid GelMA bioadhesive precursor before crosslinking may also contribute to the strength of adhesion.[55] A previously reported formulation of GelMA used as an injectable hydrogel has been studied in the context of an infarct model.[26] This older version of GelMA was not designed to adhere to tissue and was therefore delivered via intramyocardial injection. Placement of the bioadhesive on the epicardial surface, where light exposure can be consistently controlled, facilitates more precise control over the photo–crosslinking process. This is thought to lead to formation of a stronger scaffold and stronger scaffold-tissue crosslinking.

On the basis of these in vitro and ex vivo data, we hypothesized that GelMA bioadhesive could be successfully photo–crosslinked to injured myocardium in the context of a mouse model of MI (Figure 3). Epicardial application of GelMA bioadhesive had no impact on intraprocedural mortality during experimental MI (Table 1) and was associated with significantly lower mortality during the 3-week observation period after MI (Table 1). Postmortem inspection of mice that did not survive the 3-week monitoring period revealed evidence that LV rupture was the cause of death. It is therefore likely that GelMA treatment reduced post-MI mortality by preventing LV free wall rupture. In addition, GelMA-treated mice that survived the 3-week monitoring period exhibited improved LV function (Figure 4, Table 2) and reduced scar burden (Figure 5), compared with untreated mice.

Immunostaining confirmed that GelMA treatment reduced scar burden and disruption of LV architecture following MI (Figure 6A through 6C). Epicardial application of GelMA led to the preservation of CMs in the infarcted tissue without an observed increase in infiltration of macrophages or other evidence of inflammation in the infarcted territory (Figure 6E and 6F). Preservation of CMs and myocardial integrity in the infarcted territory is thought to be responsible for the improvement of LV systolic function following GelMA treatment. In other animal models, hydrogels containing a different version of GelMA and/or extracellular matrix proteins were shown to reduce post-MI scar burden and improve LV function.[56,57] Use of an extracellular matrix-based hydrogel in humans after MI resulted in improved ventricular function.[58]

Previously reported data suggest that the physical reinforcement provided by hydrogel scaffolds may not be sufficient to prevent negative remodeling after MI.[13,59] The data in this study expand on the observed improvement in LV function associated with intravascular delivery of fibrin-based nanogels in a mouse model of MI.[60] The reduced scar burden observed with epicardial GelMA application after MI suggests that GelMA may generate a biomimetic scaffold. Although GelMA was shown to be biocompatible with several cardiac cell types (CMs and CFs) in vitro, further studies will be required to assess endogenous cell growth with epicardial GelMA application in vivo.

CONCLUSIONS

We concluded that the visible light crosslinked GelMA system described in this study constitutes a rapid and controlled strategy to deliver a supportive scaffold to the site of myocardial injury. The magnitude of the effect observed in this study suggests that GelMA may be a useful system for the future study of molecular signals in the post-MI injury response. It is anticipated that this biocompatible, biodegradable hydrogel will ultimately be capable of being delivered percutaneously using a map-guided system for epicardial injection. In addition, the GelMA system used in this study was designed to maintain structural integrity for 14 days after crosslinking to both provide mechanical support and, in the

future, provide a platform for the delivery of drug or cell therapies.

Limitations

The experimental infarct model involved permanent coronary artery ligation. Therefore, the observed results may not be generalizable to other models of myocardial injury, such as ischemia-reperfusion. Additional studies will be required to determine whether the GelMA hydrogel formulation can facilitate endogenous cell proliferation, the sustained delivery of therapeutic agents (eg, drugs, cells) to injured myocardium, or both with the aim of preserving or restoring normal cardiac function following MI.

ARTICLE INFORMATION

Affiliations

From the Cardiac Arrhythmia Service (L.M.P., R.P.L., X.Y., P.A.L., J.N.R.) and Cardiovascular Research Center (C.X., J.R.), Massachusetts General Hospital, Boston, MA; Department of Chemical Engineering, Northeastern University, Boston, MA (R.P.L., E.S.S., C.H.Y., N.A.); Department of Chemical and Biomolecular Engineering (E.S.S., N.A.) and Center for Minimally Invasive Therapeutics, California NanoSystems Institute (N.A.), University of California, Los Angeles, CA.

Sources of Funding

Disclosures

None.

REFERENCES

1. Swirski F, Nahrendorf M. Leukocyte behavior in atherosclerosis, myocardial infarction, and heart failure. *Science*. 2013;339:161–166.
2. Frangogiannis N. The inflammatory response in myocardial injury, repair, and remodelling. *Nat Rev Cardiol*. 2014;5:255–265.
3. Mann D. Innate immunity and the failing heart: the cytokine hypothesis revisited. *Circ Res*. 2015;116:1254–1268.
4. King K, Aguirre A, Ye Y, Sun Y, Roh J, Ng RJ, Kohler R, Arlauckas S, Iwamoto Y, Savol A, et al. IRF3 and type I interferons fuel a fatal response to myocardial infarction. *Nat Med*. 2017;12:1481–1487.
5. Heusch G, Gersh B. The pathophysiology of acute myocardial infarction and strategies of protection beyond reperfusion: a continual challenge. *Eur Heart J*. 2017;38:774–784.
6. Hsieh J, Hsieh M, Chen C, Wang C, Chang S, Lee C, Chen D, Yang C, Tsai M. Comparison of the acute and long-term outcomes of patients with multivessel coronary artery disease after angiographic complete and incomplete revascularization with drug-eluting stents. *Circ J*. 2018;82:992–998.
7. Kenkre T, Malhotra P, Johnson B, Handberg E, Thompson D, Marroquin O, Rogers W, Pepine C, Bairey Merz C, Kelsey S. Ten-year mortality in the WISE study (Women's Ischemia Syndrome Evaluation). *Circ Cardiovasc Qual Outcomes*. 2017;10:e0033863.
8. Bangalore S, Guo Y, Samadashvili Z, Blecker S, Xu J, Hannan E. Everolimus-eluting stents or bypass surgery for multivessel coronary disease. *N Engl J Med*. 2015;372:1213–1222.
9. Bui A, Horwich T, Fonarow G. Epidemiology and risk profile of heart failure. *Nat Rev Cardiol*. 2011;8:30–41.
10. Hall M, Dondo T, Yan A, Mamas M, Timmis A, Deanfield J, Jernberg T, Hemingway H, Fox K, Gale C. Multimorbidity and survival for patients with acute myocardial infarction in England and Wales: latent class analysis of a nationwide population-based cohort. *PLoS Med*. 2018;15:e1002501.
11. Annabi N, Nichol J, Zhong X, Ji C, Koshy S, Khademosseini A, Dehghani F. Controlling the porosity and microarchitecture of hydrogels for tissue engineering. *Tissue Eng Part B Rev*. 2010;16:371–383.
12. Annabi N, Tamayol A, Uquillas J, Akbari M, Bertassoni L, Cha C, Camci-Unal G, Dokmeci M, Peppas N, Khademosseini A. Rational design and applications of hydrogels in regenerative medicine. *Adv Mater*. 2014;26:85–124.
13. Saludas L, Pascual-Gil S, Prosper F, Garbayo E, Blanco-Prieto M. Hydrogel based approaches for cardiac tissue engineering. *Int J Pharm*. 2017;523:454–475.
14. Wang W, Tan B, Chen J, Bao R, Zhang X, Liang S, Shang Y, Liang W, Cui Y, Fan G, et al. An injectable conductive hydrogel encapsulating plasmid DNA-eNOs and ADSCs for treating myocardial infarction. *Biomaterials*. 2018;160:69–81.
15. Wang L, Liu Y, Chung J, Wang T, Gaffey A, Lu M, Cavanaugh C, Zhou S, Kanade R, Atluri P, et al. Local and sustained miRNA delivery from an injectable hydrogel promotes cardiomyocyte proliferation and functional regeneration after ischemic injury. *Nat Biomed Eng*. 2017;1:983–992.
16. Fan Z, Fu M, Xu Z, Zhang B, Li Z, Li H, Zhou X, Liu X, Duan Y, Lin P, et al. Sustained release of a peptide-based matrix metalloproteinase-2 inhibitor to attenuate adverse cardiac remodeling and improve cardiac function following myocardial infarction. *Biomacromol*. 2017;18:2820–2829.
17. Chen G, Ren J, Deng Y, Wu X, Huang J, Wang G, Zhao Y, Li J. An injectable, wound-adapting, self-healing hydrogel for fibroblast growth factor 2 delivery system in tissue repair applications. *J Biomed Nanotechnol*. 2017;13:1660–1672.
18. Ichihara Y, Kaneko M, Yamahara K, Koulouroudias M, Sato N, Uppal R, Yamazaki K, Saito S, Suzuki K. Self-assembling peptide hydrogel enables instant epicardial coating of the heart with mesenchymal stromal cells for the treatment of heart failure. *Biomaterials*. 2018;154:12–23.
19. Tan H, Li H, Rubin J, Marra K. Controlled gelation and degradation rates of injectable hyaluronic acid-based hydrogels through a double cross-linking strategy. *J Tissue Eng Regen Med*. 2011;5:790–797.
20. Mathew A, Uthaman S, Cho K, Cho C, Park I. Injectable hydrogels for delivering biotherapeutic molecules. *Int J Biol Macromol*. 2018;110:17–29.
21. El-Sherbiny I, Yacoub M. Hydrogel scaffolds for tissue engineering: progress and challenges. *Glob Cardiol Sci Pract*. 2013;3:316–342.
22. Duarte A, Coelho J, Bordado J, Cidade M, Gil M. Surgical adhesives: systematic review of the main types and development forecast. *Prog Polym Sci*. 2012;37:1031–1050.
23. O'Connell C, Zhang B, Onofrillo C, Duchi S, Blanchard R, Quigley A, Bourke J, Ghambir S, Kapsa R, DiBella C, et al. Tailoring the mechanical properties of gelatin methacryloyl hydrogels through manipulation of the photocrosslinking conditions. *Soft Matter*. 2018;14:2142–2151.
24. Nguyen K, West J. Photopolymerizable hydrogels for tissue engineering applications. *Biomaterials*. 2002;23:4307–4314.
25. Basu A. DNA damage, mutagenesis and cancer. *Int J Mol Sci*. 2018;19:E970.
26. Noshadi I, Hong S, Sullivan K, Shirzaei Sani E, Portillo-Lara R, Tamayol A, Shin S, Gao A, Stoppel W, Black L, et al. In vitro and in vivo analysis of visible light crosslinkable gelatin methacryloyl (GelMA) hydrogels. *Biomater Sci*. 2017;5:2093–2105.
27. Naahidi S, Jafari M, Logan M, Wang Y, Yuan Y, Bae H, Dixon B, Chen P. Biocompatibility of hydrogel-based scaffolds for tissue engineering applications. *Biotechnol Adv*. 2017;35:530–544.
28. Yue K, Trujillo-de Santiago G, Alvarez M, Tamayol A, Annabi N, Khademhosseini A. Synthesis, properties, and biomedical applications of gelatin methacryloyl (GelMA) hydrogels. *Biomaterials*. 2015;73:254–271.
29. Hillel A, Unterman S, Nahas Z, Reid B, Coburn J, Axelman J, Chae J, Guo Q, Trow R, Thomas A, et al. Photoactivated composite biomaterial for soft tissue restoration in rodents and in humans. *Sci Transl Med*. 2011;3:93ra67.

30. Ullmann Y, Elkhatib R, Fodor L. The aesthetic applications of intense pulsed light using the Lumenis M-22 device. *Laser Ther.* 2011;20:23–28.

31. Bryant S, Nuttelman C, Anseth K. Cytocompatibility of UV and visible light photoinitiating systems on cultured NIH 3T3 fibroblasts in vitro. *J Biomater Sci Polym Ed.* 2000;11:439–457.

32. Lin H, Zhang D, Alexander P, Yang G, Tan G, Cheng A, Tuan R. Application of visible light-based projection stereolithography for live cell-scaffold fabrication with designed architecture. *Biomaterials.* 2013;34:331–339.

33. Nichol J, Koshy S, Bae H, Hwang C, Yamanlar S, Khademhosseini A. Cell-laden microengineered gelatin methacrylate hydrogels. *Biomaterials.* 2010;31:5536–5544.

34. Annabi N, Rana D, Shirzaei Sani S, Portillo-Lara R, Gifford J, Fares M, Mithieux S, Weiss A. Engineering a sprayable and elastic hydrogel adhesive with antimicrobial properties for wound healing. *Biomaterials.* 2017;139:229–243.

35. Noshadi I, Walker B, Portillo-Lara R, Shirzaei Sani E, Gomes N, Aziziyan M, Annabi N. Engineering biodegradable and biocompatible bio-ionic liquid conjugated hydrogels with tunable conductivity and mechanical properties. *Sci Rep.* 2017;7:4345.

36. Li J, Celiz A, Yang J, Yang Q, Wamala I, Whyte W, Seo B, Vasilyev N, Vlassak J, Suo Z, et al. Tough adhesives for diverse wet surfaces. *Science.* 2017;357:378–381.

37. Annabi N, Shin S, Tamayol A, Miscuglio M, Bakooshli M, Assmann A, Mostafalu P, Sun J-Y, Mithieux S, Cheung L, et al. Highly elastic and conductive human-based protein hybrid hydrogels. *Adv Mater.* 2016;28:40–49.

38. Annabi N, Tsang K, Mithieux S, Nikkhah M, Ameri A, Khademhosseini A, Weiss A. Highly elastic micropatterned hydrogel for engineering functional cardiac tissue. *Adv Funct Mater.* 2013;23:4950–4959.

39. Takagawa J, Zhang Y, Wong M, Sievers R, Kapasi N, Wang Y, Yeghiazarians Y, Lee R, Grossman W, Springer M. Myocardial infarct size measurement in the mouse chronic infarction model: comparison of area- and length-based approaches. *J Appl Physiol.* 1985;102:2104–2111.

40. Van Craeyveld E, Jacobs F, Gordts S, De Geest B. Low-density lipoprotein receptor gene transfer in hypercholesterolemic mice improves cardiac function after myocardial infarction. *Gene Ther.* 2012;19:860–871.

41. Hiesinger W, Brukman M, McCormick R, Fitzpatrick J III, Frederick J, Yang E, Muenzer J, Marotta N, Berry M, Atluri P, et al. Myocardial tissue elastic properties determined by atomic force microscopy after stromal cell-derived factor 1alpha angiogenic therapy for acute myocardial infarction in a murine model. *J Thorac Cardiovasc Surg.* 2012;143:962–966.

42. Annabi N, Yue K, Tamayol A, Khademhosseini A. Elastic sealants for surgical applications. *Eur J Pharm Biopharm.* 2015;95(part A):27–39.

43. Bouten P, Zonjee M, Bender J, Yauw S, van Goor H, van Hest J, Hoogenboom R. The chemistry of adhesive materials. *Prog Polym Sci.* 2014;39:1375–1405.

44. Singer A, Quinn J, Hollander J. The cyanoacrylate topical skin adhesives. *Am J Emerg Med.* 2008;26:490–496.

45. Montanaro L, Arciola C, Cenni E, Ciapetti G, Savioli F, Filippini F, Barsanti L. Cytotoxicity, blood compatibility and antimicrobial activity of two cyanoacrylate glues for surgical use. *Biomaterials.* 2001;22:59–66.

46. Vakalopoulos K, Wu Z, Kroese L, Kleinrensink G, Jeekel J, Vendamme R, Dodou D, Lange J. Mechanical strength and rheological properties of tissue adhesives with regard to colorectal anastomosis: an ex vivo study. *Ann Surg.* 2015;261:323–331.

47. Sierra D, Eberhardt A, Lemons J. Failure characteristics of multiple-component fibrin-based adhesives. *J Biomed Mater Res.* 2002;59:1–11.

48. Yang J, Bai R, Suo Z. Topological adhesion of wet materials. *Adv Mater.* 2018;30:e1800671.

49. Elvin C, Vuocolo T, Brownlee A, Sando L, Huson M, Liyou N, Stockwell P, Lyons R, Kim M, Edwards G, et al. A highly elastic tissue sealant based on photopolymerised gelatin. *Biomaterials.* 2010;31:8323–8331.

50. Kim H, Park W. Chemically cross-linked silk fibroin hydrogel with enhanced elastic properties, biodegradability, and biocompatability. *Int J Nanomedicine.* 2016;11:2967–2978.

51. Lang N, Pereira M, Lee Y, Friehs I, Vasilyev N, Feins E, Ablasser K, O'Cearbhaill E, Xu C, Fabozzo A, et al. A blood-resistant surgical glue for minimally invasive repair of vessels and heart defects. *Sci Transl Med.* 2014;6:218ra6.

52. Annabi N, Zhang Y, Assmann A, Sani E, Cheng G, Lassaletta A, Vegh A, Dehghani B, Ruiz-Esparza G, Wang X, et al. Engineering a highly elastic human protein-based sealant for surgical applications. *Sci Transl Med.* 2017;9:eaai7466.

53. Krzemiński T, Nozyński J, Grzyb J, Porc M. Wide-spread myocardial remodeling after acute myocardial infarction in rat: features for heart failure progression. *Vascul Pharmacol.* 2008;48:100–108.

54. Assmann A, Vegh A, Ghasemi-Rad M, Bagherifard S, Cheng G, Sani E, Ruiz-Esparza G, Noshadi I, Lassaletta A, Ganghadaran S, et al. A highly adhesive and naturally derived sealant. *Biomaterials.* 2017;140:115–127.

55. Mehdizadeh M, Yang J. Design strategies and applications of tissue bioadhesives. *Macromol Biosci.* 2013;13:271–288.

56. Bejleri D, Streeter B, Nachias A, Brown M, Gaetani R, Christman K, Davis M. A bioprinted cardiac patch composed of cardiac-specific extracellular matrix and progenitor cells for heart repair. *Adv Healthc Mater.* 2018;7:e1800672.

57. Singelyn J, Sundaramurthy P, Johnson T, Schup-Magoffin P, Hu D, Faulk D, Wang J, Mayle K, Bartels K, Salvatore M, et al. Catheter-deliverable hydrogel derived from decellularized ventricular extracellular matrix increases endogenous cardiomyocytes and preserves cardiac function post-myocardial infarction. *J Am Coll Cardiol.* 2012;59:751–763.

58. Traverse J, Henry T, Dib N, Patel A, Pepine C, Schaer G, DeQuach J, Kinsey A, Chamberlin P, Christman K. First-in-man study of a cardiac extracellular matrix hydrogel in early and late myocardial infarction patients. *JACC Basic Transl Sci.* 2019;4:659–669.

59. Rane A, Chuang J, Shad A, Hu D, Dalton N, Gu Y, Peterson K, Omens J, Christman K. Increased infarct wall thickness by a bio-inert material is insufficient to prevent negative left ventricular remodeling after myocardial infarction. *PLoS One.* 2011;6:e21571.

60. Mihalko E, Huang K, Sproul E, Cheng K, Brown A. Targeted treatment of ischemic and fibrotic complications of myocardial infarction using a dual-delivery microgel therapeutic. *ACS Nano.* 2018;12:7826–7837.